nature structural & molecular biology

A new MCM modification cycle regulates DNA replication initiation

Lei Wei[1,2] & Xiaolan Zhao[1]

The MCM DNA helicase is a central regulatory target during genome replication. MCM is kept inactive during G1, and it initiates replication after being activated in S phase. During this transition, the only known chemical change to MCM is the gain of multisite phosphorylation that promotes cofactor recruitment. Because replication initiation is intimately linked to multiple biological cues, additional changes to MCM can provide further regulatory points. Here, we describe a yeast MCM SUMOylation cycle that regulates replication. MCM subunits undergo SUMOylation upon loading at origins in G1 before MCM phosphorylation. MCM SUMOylation levels then decline as MCM phosphorylation levels rise, thus suggesting an inhibitory role of MCM SUMOylation during replication. Indeed, increasing MCM SUMOylation impairs replication initiation, partly through promoting the recruitment of a phosphatase that decreases MCM phosphorylation and activation. We propose that MCM SUMOylation counterbalances kinase-based regulation, thus ensuring accurate control of replication initiation.

The initiation of DNA replication is tightly controlled to ensure that duplication of every locus occurs once and only once per cell cycle and to establish specific replication programs unique to an organism or cell type. Impairment in regulation of replication initiation can lead to various forms of genomic changes and instability, and consequently to human diseases and cancers[1–5]. Previous studies have revealed multiple forms of regulation at both local and global levels, including several pathways targeting a key replicative enzyme, the DNA helicase MCM[4,6–12].

The MCM complex is composed of Mcm2–7 subunits and is highly conserved in eukaryotes. Among its many roles during replication, MCM is critical for replisome assembly. MCM, in complex with cofactor Cdt1, is the first replisome component to arrive at replication initiation sites (or origins). In budding yeast, MCM loading at origins is mediated by Cdc6 and the origin recognition complex (ORC, comprising Orc1–6) in late mitosis and G1 phase, in a process called origin licensing[13,14] (**Fig. 1a**). A subset of loaded MCM then initiates stepwise replisome assembly in a process termed origin firing. This begins with the recruitment of two cofactors: Cdc45 and the heterotetrameric GINS complex (**Fig. 1a**). Recruitment of both factors requires kinases. Dbf4-dependent kinase (DDK, composed of Cdc7 and Dbf4) primarily phosphorylates Mcm4, thereby recruiting Cdc45; subsequent phosphorylation of non-MCM proteins by the S-phase cyclin-dependent kinase complex (S-CDK) recruits GINS[13–16] (**Fig. 1a**). The Cdc45, MCM and GINS (CMG) complex serves as the replicative helicase[13,14]. After CMG formation, more than a dozen additional replisome members assemble in a highly ordered yet still poorly understood manner before replication is initiated[13,14,17,18]. Throughout this intricate replisome-assembly process, MCM and CMG are kept inactive to prevent premature DNA unwinding.

The precision of many biological processes depends on the balance between positive and negative regulation. It is conceivable that the tightly controlled transition from inactive to active MCM states also requires additional regulation besides the known kinase-based positive regulation. Recent studies have indeed revealed other chemical modifications of MCM. In particular, proteomic screens in yeast, humans and plants have shown that MCM subunits are SUMOylated, thus revealing another highly conserved MCM modification[19–21]. SUMOylation entails the conjugation of the small protein modifier SUMO to lysine residues on target proteins. This modification is reversible through deSUMOylation, and the cycle of SUMOylation and deSUMOylation is highly dynamic in cells. The addition and removal of SUMO exert a range of effects on protein function, such as altering protein-protein interactions or enzymatic activities, and influence a variety of cellular processes[22,23]. Although SUMO is known to affect genome maintenance, its roles in this arena have been examined primarily under genome-damaging situations[19,24–28]; how SUMO influences the normal replication program is largely unanswered.

To understand how SUMOylation of MCM subunits pertains to normal replication programs, we first examined spatial and temporal patterns of this modification in budding yeast. We found that SUMOylation of the six MCM subunits occurred exclusively on chromatin. Moreover, MCM SUMOylation levels oscillated during the cell cycle in a manner opposite to those of MCM phosphorylation, suggesting that MCM SUMOylation is an inhibitory marker for replication. The MCM SUMOylation cycle depended on key MCM loaders

[1]Molecular Biology Program, Memorial Sloan Kettering Cancer Center, New York, New York, USA. [2]Gerstner Sloan Kettering Graduate School of Biomedical Sciences, Memorial Sloan Kettering Cancer Center, New York, New York, USA. Correspondence should be addressed to X.Z. (zhaox1@mskcc.org).

Received 23 June 2015; accepted 6 January 2016; published online 8 February 2016; doi:10.1038/nsmb.3173

and activators, suggesting that it is integral to MCM functions. Importantly, increased MCM SUMOylation impaired replication initiation and decreased CMG levels. Mechanistically, these effects were linked to enhanced recruitment of the phosphatase PP1, which counteracts DDK functions. Together, our findings suggest that MCM SUMOylation enables a form of negative regulation during replication initiation. We propose that the dual control of MCM by two modifications ensures precise replication initiation and enables flexible control of genome duplication under different cellular contexts.

RESULTS

Detection of MCM-subunit SUMOylation during normal growth

In search of additional means of MCM regulation, we investigated MCM SUMOylation, which has been found in proteomic screens in multiple organisms[19–21]. To detect SUMOylation, we followed a well-established method wherein denaturing conditions throughout protein preparation are used to minimize deSUMOylation[29]. In this method, the endogenous yeast SUMO (Smt3) is replaced with a hexahistidine (His_6)-Flag–tagged version (HF-Smt3) at its genomic locus, such that SUMOylated forms containing HF-Smt3 are enriched by Ni-NTA resin (referred to herein as Ni PD). Although unmodified forms of proteins show nonspecific histidine-mediated binding to Ni-NTA, they can be distinguished from SUMOylated forms upon western blotting for a particular protein on the basis of two criteria: (i) SUMOylated forms are detected only in the presence of HF-Smt3 but not untagged Smt3, whereas unmodified forms are detectable regardless of the presence of HF-Smt3, and (ii) mono-SUMOylated forms show an ~20-kDa upshift compared to the unmodified forms.

In our tests, we tagged Mcm2–7 proteins with hemagglutinin (HA) at their endogenous loci and verified that cell growth was fully supported by the tagged proteins. In the presence of HF-Smt3, but not untagged Smt3, we detected a modified form of each MCM subunit with anti-HA antibodies through western blotting (**Fig. 1b**). In each case, the modified form exhibited an ~20-kDa upshift from the unmodified form of the protein (**Fig. 1b**). Consistently with their being the SUMOylated species, these modified forms showed a smaller upshift when SUMO was tagged with a smaller tag (**Supplementary Fig. 1a**). We also observed SUMOylated forms of each MCM subunit when examining immunoprecipitated protein by western blotting with SUMO-specific antibodies (**Supplementary Fig. 1b**). In all cases, the detected levels of MCM SUMOylation were not abundant, consistently with the dynamic nature of this modification. After showing through two approaches that a fraction of each MCM subunit was SUMOylated during normal growth, we used the Ni PD method in subsequent tests.

MCM SUMOylation on chromatin requires its loading at origins

Because MCM is subject to tight spatial regulation and can function only upon chromatin loading, we asked whether the chromatin-bound or soluble fraction of MCM was SUMOylated. SUMOylated MCM subunits were detectable exclusively in the chromatin-bound fraction (**Fig. 1c**). Consistently with this finding, MCM-subunit SUMOylation was absent when MCM loading onto chromatin was prevented by Cdc6 depletion in G1 cells (**Fig. 1d** and **Supplementary Fig. 2a**). These results suggest that MCM-subunit SUMOylation occurs on chromatin after the complex is loaded at origins.

MCM SUMOylation levels peak in G1 and decline in S phase

Next, we examined the temporal regulation of MCM SUMOylation during the cell cycle. We arrested cells in G1 and then allowed them to synchronously progress through the cell cycle (**Fig. 2a**, fluorescence-activated cell sorting (FACS)). Using Mcm6 as an example, we observed an oscillation in SUMOylation levels: SUMOylation of Mcm6 peaked in G1 phase, coinciding with its chromatin loading, declined during S phase and reappeared in M phase, concurrently with the next loading cycle (**Fig. 2a**). Examination of chromatin-bound Mcm6 also showed a high SUMOylation level in G1 and a low level in S phase (**Supplementary Fig. 2b**).

We observed similar patterns for Mcm2–5, detecting SUMOylation in G1 when DDK activity, as indicated by Mcm4 phosphorylation, and

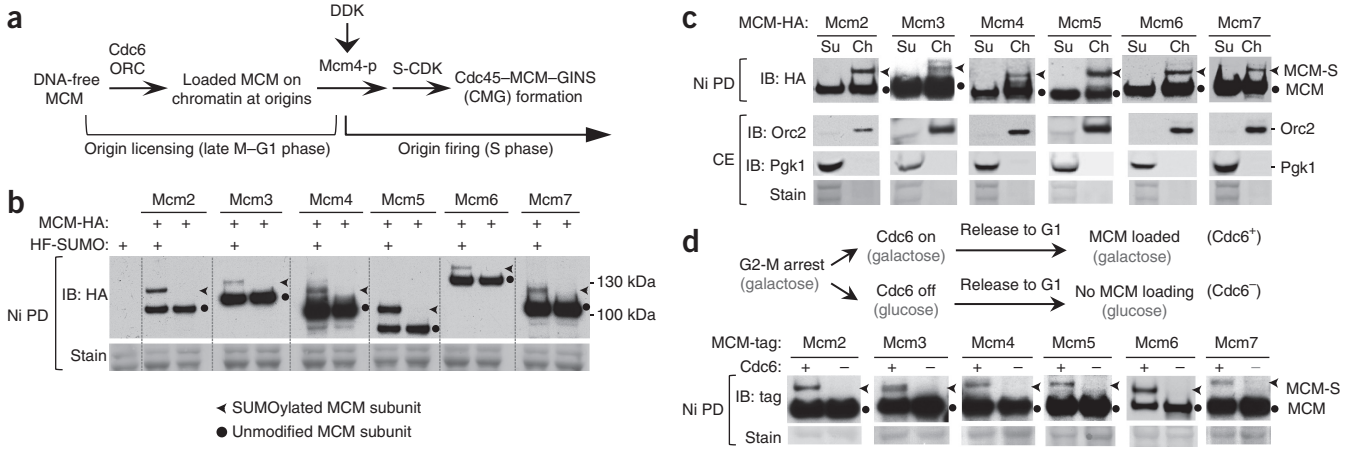

Figure 1 SUMOylation of six MCM subunits occurs on chromatin and is dependent on MCM loading at replication origins. (**a**) Scheme of key events for MCM loading and activation (details in main text). Mcm4-p, phosphorylated Mcm4; S-CDK, S cyclin–dependent kinase; DDK, Dbf4-dependent kinase. (**b**) Immunoblots (IB) showing mono-SUMOylation of each MCM subunit under normal growth conditions. HF-SUMO, His_6-Flag–tagged SUMO; MCM-HA, HA-tagged MCM. Unmodified (MCM) and SUMOylated (MCM-S) bands are indicated by dots and arrowheads, respectively. Equal protein loading is shown by Ponceau S staining (stain). Similar methods and annotations are used subsequently. (**c**) Immunoblots showing SUMOylation of only chromatin-bound MCM subunits. Samples are HA-tagged MCM subunits examined in chromatin-bound (Ch) and supernatant (Su) fractions and Ni PD tests. Orc2 and Pgk1 are markers for chromatin and supernatant fractions of cell extracts (CE), respectively. (**d**) Top, experimental scheme for Cdc6 depletion and prevention of MCM loading, as described previously[37]. Bottom, immunoblots showing SUMOylation status of MCM subunits in the presence (+) or absence (–) of Cdc6. Mcm5 was tagged with Strep tag II to be compatible with the Gal-Cdc6 construct, and other MCM subunits were tagged with HA. Validation of Cdc6 depletion and G1 arrest is shown in **Supplementary Figure 2a**.

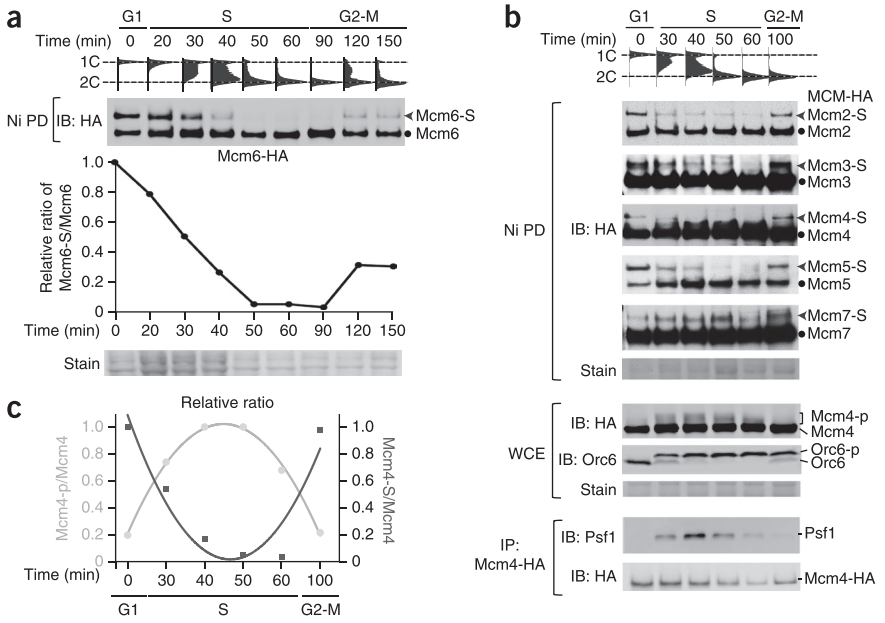

Figure 2 SUMOylation levels of MCM subunits oscillate during the cell cycle. (**a**) Top, flow cytometry profiles showing cell-cycle progression from G1 to S and G2-M phases. 1C and 2C indicate the genome size. Middle, immunoblot showing SUMOylation levels of HA-tagged Mcm6 at the indicated time points. The graph depicts the relative ratio of SUMOylated to unmodified Mcm6 on the immunoblot, with the ratio in G1 cells set to 1. Stain at the bottom shows protein loading. (**b**) Flow cytometry profiles as in **a**, showing cell-cycle progression. Immunoblots of Ni PD samples show the SUMOylation status of HA-tagged MCM subunits at the indicated time points; immunoblots of cell extracts (WCE) show the levels of Mcm4 phosphorylation (Mcm4-p) and Orc6 phosphorylation (Orc6-p); immunoblots of immunoprecipitated samples show Mcm4-bound Psf1. (**c**) Plot showing the relative ratios of SUMOylated or phosphorylated Mcm4 to unmodified Mcm4 levels. The ratio was calculated from results in **b**, and the highest value was set to 1.

CDK activity, as indicated by Orc6 phosphorylation, were low (**Fig. 2b**). As expected, CMG levels were also low in G1, as evidenced by the low amount of the GINS subunit Psf1 associated with Mcm4 (**Fig. 2b**). As cells entered S phase, DDK and CDK activities, as well as CMG levels, rose (**Fig. 2b**), whereas Mcm2–5 SUMOylation levels decreased (**Fig. 2b**). In G2-M phase, when DDK and CDK activities, as well as CMG levels fell, SUMOylation levels of Mcm2–5 rose again (**Fig. 2b**). The Mcm7 SUMOylation pattern was somewhat different. Like other MCM subunits, Mcm7 showed SUMOylation in G1; however, unlike that of other MCM subunits, Mcm7 SUMOylation persisted throughout most of S phase, then decreased in late S phase and reappeared in G2-M phase (**Fig. 2b**). The difference in SUMOylation patterns between Mcm2–6 and Mcm7 may reflect distinct regulation and functions.

Together, SUMOylation levels of Mcm2–6 oscillate during the cell cycle in a pattern opposite to those of DDK- and CDK-mediated phosphorylation events. We also visualized this phenomenon by plotting the relative ratio of SUMOylated or phosphorylated Mcm4 versus unmodified Mcm4 proteins (**Fig. 2c**). This temporal pattern suggests that in contrast to phosphorylation, MCM SUMOylation is an inhibitory marker of replication initiation.

MCM SUMOylation loss in S phase requires DDK and GINS

To gain a detailed understanding of the changes in Mcm2–6 SUMOylation at the G1-S transition, we examined the roles of two key MCM regulators, DDK and GINS. To test the role of DDK, we arrested cells containing the temperature-sensitive *cdc7-4* allele and HA-tagged MCM subunits in G1 at a permissive temperature (24 °C) and then shifted them to a nonpermissive temperature (37 °C) before releasing them into S phase (**Fig. 3a**). We confirmed *cdc7-4* inactivation upon temperature shift, on the basis of the lack of Mcm4 phosphorylation (**Supplementary Fig. 2c**). We found that SUMOylation of Mcm2–6 still occurred in G1 when DDK was inactivated and that the Mcm6 SUMOylation level was similar to that in wild-type cells (**Fig. 3a**). Thus, bulk MCM SUMOylation in G1 did not require DDK. However, DDK inactivation prevented the loss

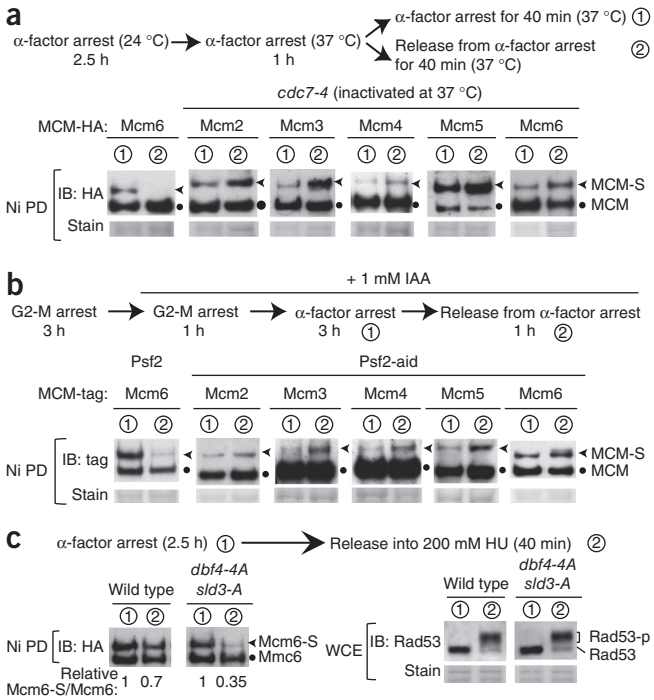

Figure 3 Loss of Mcm2–6 SUMOylation at the G1-S transition requires DDK, GINS and replication initiation. (**a**) Top, experimental scheme showing Cdc7 inactivation in G1 phase (alpha-factor arrest, 37 °C) followed by either continued G1 arrest or release from arrest, as described previously[38] (Online Methods). Bottom, immunoblots showing the SUMOylation status of HA-tagged MCM subunits at the indicated time points in the experimental scheme. (**b**) Top, experimental scheme for Psf2 depletion after cell synchronization at G2-M phase, G1 arrest and subsequent release (Online Methods). Bottom, immunoblots showing the SUMOylation status of each MCM subunit at the indicated time points in the experimental scheme. Mcm5 was tagged with Strep tag II to be compatible with the Psf2-aid construct, and other MCM subunits were tagged with HA. (**c**) Top, experimental scheme for G1 arrest and release. Bottom, immunoblots showing Mcm6 SUMOylation status (left) and Rad53 phosphorylation (Rad53-p) at indicated time points in the experimental scheme.

of Mcm2–6 SUMOylation when G1 cells were released into S phase (**Fig. 3a**). This effect was not due to indirect alteration of CDK activity (as monitored by Orc6 phosphorylation) or DNA damage–checkpoint activity (monitored by Rad53 phosphorylation) (**Supplementary Fig. 2c**). Thus, DDK is required for loss of Mcm2–6 SUMOylation when cells enter S phase.

To test the role of GINS, we used an indole-3-acetic acid (IAA)-inducible degron (aid) method to acutely deplete the GINS subunit Psf2 (refs. 30,31). We arrested Psf2-aid and control cells in G2-M phase, and Psf2-aid was degraded after IAA addition (**Fig. 3b** and **Supplementary Fig. 2d**,**e**). Next, we released cells into G1 arrest in the presence of IAA and subsequently allowed them to enter S phase (**Fig. 3b**; efficient Psf2-aid degradation, proper cell-cycle arrest and release, and expected lethality caused by Psf2 degradation are shown in **Supplementary Fig. 2d**–**f**). As in the case for DDK, Psf2 loss did not affect Mcm2–6 SUMOylation in G1 but prevented Mcm2–6 SUMOylation loss (**Fig. 3b**). The observed effects were not due to a lack of CDK and DDK activities or abnormal checkpoint activation (**Supplementary Fig. 2e**).

Together, these results show that DDK and GINS are not required for Mcm2–6 SUMOylation in G1; instead, they are required for the loss of this modification at the beginning of S phase. These findings, in conjunction with the cell-cycle pattern of Mcm2–6 SUMOylation, suggest that the modification takes place before DDK- and GINS-mediated events and then decreases in a DDK- and GINS-dependent manner upon S-phase entry.

Mcm6 SUMOylation loss coincides with origin firing

Next, we addressed how the change in Mcm2–6 SUMOylation status at the G1-S transition is related to early and late origin firing. Releasing G1 cells into medium containing 200 mM hydroxyurea (HU) for a short time (for example, 60 min) allows limited DNA synthesis from early origins[32]. The number of fired origins greatly increases when checkpoint-mediated inhibition of late origins is removed by mutating the phosphorylation sites on the DDK subunit Dbf4 and the replisome-assembly factor Sld3 (*dbf4-4A sld3-A*)[33]. Thus, releasing G1 cells into HU-containing medium for a short time allows the assessment of the influence of firing of only early origins (in wild-type cells) versus both early and late origins (in *dbf4-4A sld3-A* cells).

Using this experimental setup, we found that 40 min after release into HU, the Mcm6 SUMOylation level was reproducibly decreased by approximately 30% in wild-type and 65% in *dbf4-4A sld3-A* cells, relative to the level in G1-arrested cells (**Fig. 3c**). These results suggest that loss of Mcm6 SUMOylation coincides with the firing of both early and late origins. Because wild-type and *dbf4-4A sld3-A* cells do not experience replication termination under this treatment[12], the observed Mcm6 SUMOylation loss is not associated with replication termination.

Mcm6-SuOn increases MCM SUMOylation

The correlation of Mcm2–6 SUMOylation loss with origin firing led us to hypothesize that this modification inhibits replication initiation. An important prediction of this hypothesis is that increasing MCM SUMOylation should impair replication initiation. To test this prediction, we used a tagging strategy that utilizes the high-affinity SUMO interaction region from a catalytically inactive SUMO protease domain to promote SUMOylation of its fusion partner and subunits of the same complex, presumably by increasing the local SUMO concentration[34] (**Supplementary Fig. 3a**). We fused this tag, referred to as SuOn (denoting SUMO on), to Mcm6. As a control, we fused Mcm6 to the same tag containing a point mutation of a key residue required for SUMO interaction (Mcm6-ctrl)[34,35]. Both fusions were expressed from the endogenous *MCM6* locus and tagged with the V5 epitope.

Compared with Mcm6-ctrl, Mcm6-SuOn showed an increase of at least approximately four-fold in a modified form of the protein in both G1 and S phases (**Fig. 4a**). This form exhibited the characteristic ~20-kDa upshift of mono-SUMO modification and was increased in Mcm6-SuOn cells, thus suggesting that it was the SUMOylated form (**Fig. 4a**). We validated this conclusion with two additional tests. We found that first, compared with untagged SUMO, HF-Smt3 led to a further upshift of this form (**Supplementary Fig. 3b**). Second, immunoprecipitation of Mcm6-SuOn or Mcm6-ctrl and subsequent western blotting showed that this form was recognized by a SUMO-specific antibody (**Supplementary Fig. 3c**). Together, these findings demonstrated that the modified form represented the SUMOylated form. Mcm6-SuOn also increased SUMOylation levels of three other MCM subunits (Mcm2, 4 and 7) and thus is an effective tool to increase MCM SUMOylation (**Supplementary Fig. 3d**).

Subsequent tests showed that Mcm6-SuOn did not affect the general behavior of MCM or modification of other replication factors: (i) Mcm6-SuOn mimicked Mcm6-ctrl with regard to protein level or MCM-complex formation (**Fig. 4a** and **Supplementary Fig. 3e**); (ii) Mcm6-SuOn and Mcm6-ctrl exhibited a normal distribution between

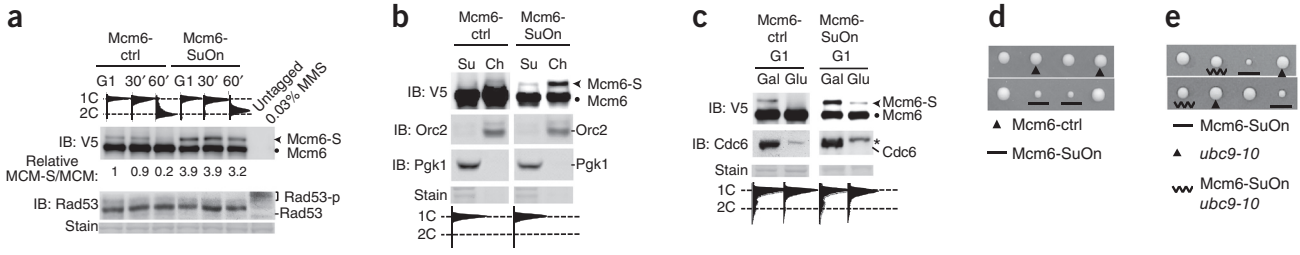

Figure 4 Increasing SUMOylation by Mcm6-SuOn slows growth, and this defect is suppressed by a *ubc9* mutant. (**a**) Top, flow cytometry profiles showing G1 arrest and subsequent release into S phase. Times in minutes (′) are indicated. Middle, immunoblot showing the SUMOylation status of V5-tagged Mcm6-ctrl and Mcm6-SuOn proteins in cell lysates. The relative ratios of SUMOylated to total Mcm6 proteins are indicated, with the ratio in the first lane set to 1. Bottom, immunoblot showing Rad53 phosphorylation (Rad53-p) and stain showing equal protein loading. The MMS-treated sample with untagged Mcm6 shows no cross-reaction bands on an anti-V5 blot (top) and robust Rad53 phosphorylation (bottom). (**b**) Immunoblots showing the SUMOylation status of Mcm6-ctrl and Mcm6-SuOn in the chromatin-bound (Ch) and supernatant (Su) fractions in G1 cells. Orc2 and Pgk1 are markers for chromatin and supernatant fractions, respectively. Bottom, flow cytometry showing G1 arrest of the samples. (**c**) Top, immunoblots showing the SUMOylation status of Mcm6-ctrl and Mcm6-SuOn in G1 cells in the presence (Gal) or absence (Glu) of Cdc6. Middle, immunoblots showing the validation of Cdc6 depletion. The experimental scheme is as in **Figure 1d**. Asterisk indicates a cross-reaction band. (**d**,**e**) Representatives of tetrads from Mcm6-SuOn/+ (bottom, 32 tetrads) or Mcm6-ctrl/+ (top, 16 tetrads) diploid strains (**d**) and Mcm6-SuOn/+ *ubc9-10*/+ diploid strains (16 tetrads) (**e**). Genotypes of spore clones are indicated.

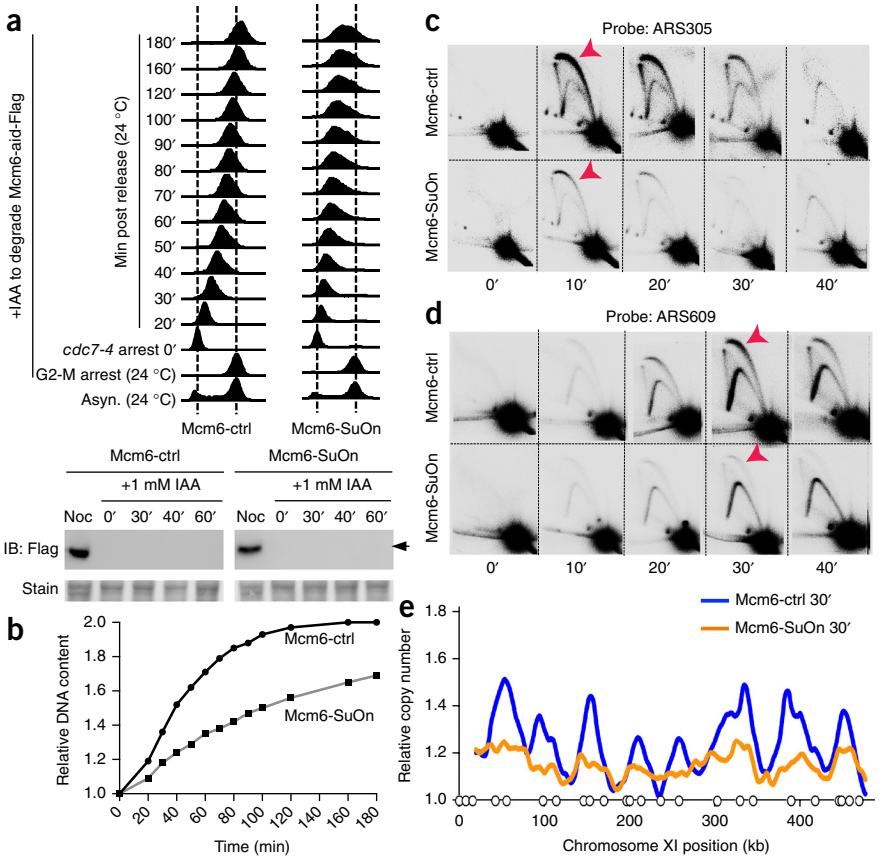

Figure 5 Mcm6-SuOn impairs replication initiation. (**a**) Top, flow cytometry analyses and experimental schemes (details in Results and Online Methods). Bottom, immunoblots showing the loss of Mcm6-aid protein (arrow) after IAA addition; stain shows equal protein loading. Asyn, asynchronous culture; noc, G2-M arrest by nocodazole. (**b**) Plot showing the relative DNA contents derived from flow cytometry analysis in **a** (Online Methods). (**c**,**d**) 2D gel results showing origin firing at ARS305 (**c**) and ARS609 (**d**), in Mcm6-ctrl and Mcm6-SuOn strains. Samples were from the same experiment as shown in **a**. Red arrowheads indicate bubble DNA structures representing origin firing events. (**e**) Plot showing relative DNA copy numbers in a section of chromosome XI, based on genome-sequencing results from 30 min post-release samples in **a**. Open circles indicate confirmed replication origins according to OriBD. Times in minutes (′) are indicated.

chromatin and cytosol factions, thus suggesting proficient chromosomal loading (**Fig. 4b**); (iii) SUMOylated Mcm6-SuOn was detected in the chromatin fraction in a Cdc6-dependent manner (**Fig. 4b**,**c**); (iv) Mcm6-SuOn did not affect SUMOylation of several other DNA-replication factors (**Supplementary Fig. 3f**); and (v) Mcm6-SuOn did not show abnormal DNA damage–checkpoint activation (**Fig. 4a**). These results suggest that the increased MCM SUMOylation caused by Mcm6-SuOn obeys the rules of MCM SUMOylation and does not perturb general MCM behavior or other replication and checkpoint protein modifications.

Mcm6-SuOn impairs replication initiation

Next, we examined how increased MCM SUMOylation by Mcm6-SuOn affected replication and growth. Mcm6-SuOn grew slowly, whereas Mcm6-ctrl supported normal growth (**Fig. 4d** and **Supplementary Fig. 4a**). Importantly, this defect was ameliorated when the SUMO E2 Ubc9 was mutated (**Fig. 4e**). Thus, although tagging *per se* did not interfere with protein functions, Mcm6-SuOn impaired growth in a SUMOylation-dependent manner.

We next examined the kinetics of S-phase progression. To avoid chronic defects caused by Mcm6-SuOn, we constructed diploid cells homozygous for *cdc7-4*, containing either Mcm6-SuOn or Mcm6-ctrl and an Mcm6-aid allele. We synchronized cells grown at the permissive temperature for *cdc7-4* (24 °C) in G2-M and then depleted Mcm6-aid by IAA addition (**Fig. 5a**). Next, we released cells from G2-M arrest and synchronized them at the G1-S boundary by raising the temperature to 37 °C to inactivate *cdc7-4*. Finally, we released cells from this arrest by bringing the temperature back to 24 °C to reactivate Cdc7-4. FACS profiles showed that cells containing Mcm6-SuOn or Mcm6-ctrl entered S phase after the final release, but Mcm6-SuOn cells exhibited a slower replication profile than that of Mcm6-ctrl cells (**Fig. 5a**). Quantification of DNA content from the FACS analyses suggested that Mcm6-SuOn cells moved through S phase about half as quickly as the control (**Fig. 5b**).

To understand whether the slow replication seen in Mcm6-SuOn cells was due to replication initiation defects, we subjected the samples collected in the above tests to two-dimensional agarose gel

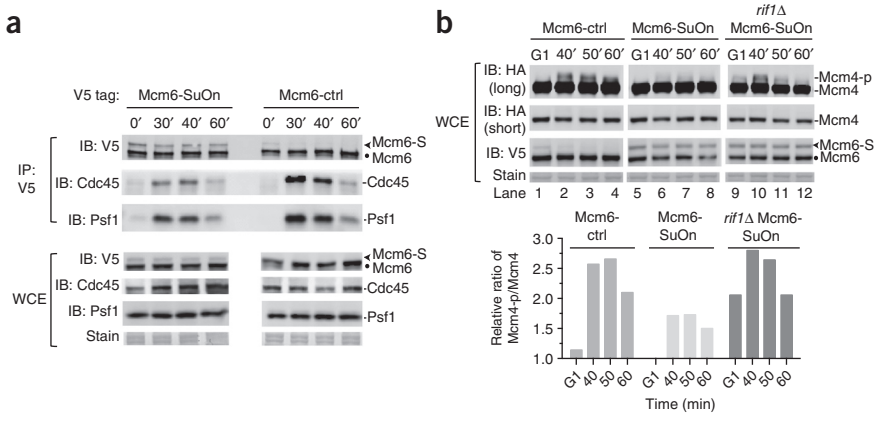

Figure 6 Low CMG levels in Mcm6-SuOn cells correlate with impaired Mcm4 phosphorylation, which is suppressed by *rif1*Δ. (**a**) Top, immunoblots showing the levels of Cdc45 and Psf1 coimmunoprecipitated with V5-tagged Mcm6-SuOn or Mcm6-ctrl. Bottom, immunoblots showing Mcm6, Cdc45 and Psf1 protein levels in the cell extracts. The experimental scheme and time points in minutes (′) are as in **Figure 5a**. (**b**) Top, immunoblots showing Mcm4 phosphorylation (long exposure) and unmodified Mcm4 protein (short exposure) for the indicated strains. Bottom, immunoblots showing Mcm6 protein levels (IB: V5) and equal loading (stain). The relative ratios of phosphorylated Mcm4 versus unmodified Mcm4 are plotted in the graph. The experimental schemes and time points are as in **Figure 2b**.

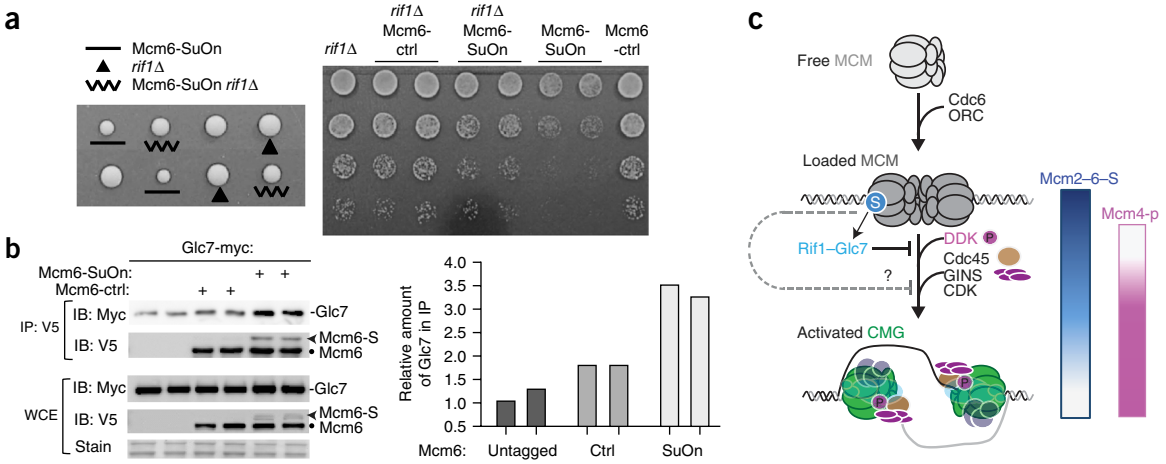

Figure 7 *rif1*Δ suppresses Mcm6-SuOn growth defects, and Mcm6-SuOn leads to enhanced association between Mcm6 and the Glc7 phosphatase. (**a**) Left, representative tetrads (from 39 total) from Mcm6-SuOn/+ *rif1*Δ/+ diploid strains. Genotypes of spore clones are indicated. Right, five-fold serial dilutions of cells spotted on plates. (**b**) Top, immunoblots (IP: V5) showing Glc7 coimmunoprecipitated with V5-tagged Mcm6-ctrl or Mcm6-SuOn in G1 cells. The first two lanes are samples with untagged Mcm6. Bottom, immunoblots showing protein levels in cell extract (WCE) and stain showing equal loading. Right, plot showing the quantification of Glc7 levels in the immunoprecipitated fraction, with the value of untagged control (first lane) set to 1. (**c**) Model depicting the spatial and temporal pattern of the MCM SUMOylation cycle and a role of MCM SUMOylation in negative regulation of replication initiation. For simplicity, only the replication factors used in this study are shown. After Cdc6-mediated MCM loading at replication origins, a fraction of Mcm2–7 subunits are SUMOylated. This occurs before DDK-mediated Mcm4 phosphorylation and CMG formation. MCM SUMOylation can then aid in recruitment of Glc7 phosphatase, thus counteracting Mcm4 phosphorylation and preventing premature CMG formation in G1. Roles for MCM SUMOylation in an event after DDK activation may be possible, as indicated by the question mark. As replication is initiated in waves, SUMOylation of Mcm2–6 decreases. The loss of Mcm2–6 SUMOylation is concomitant with the appearance of DDK-mediated Mcm4 phosphorylation, and both these events promote replication initiation.

electrophoresis (2D gel). Using probes specific to an early origin (ARS305) and a late origin (ARS609), we detected replication-firing events as bubble DNA structures, as shown previously (**Fig. 5c**,**d**). Whereas Mcm6-ctrl cells showed robust origin-firing signals at both loci at the expected times, Mcm6-SuOn cells showed weaker signals, thus indicating impaired replication initiation (**Fig. 5c**,**d**).

From deep-sequencing analysis of samples from *cdc7-4* arrest (0 min) and 30 min after release, we deduced copy-number changes and genome-wide replication profiles[38]. This analysis showed that Mcm6-SuOn cells, compared with Mcm6-ctrl cells, exhibited decreased replication at nearly all the origins annotated in the DNA Replication Origin Database (OriDB) (**Fig. 5e** and **Supplementary Fig. 5**). Together, these results demonstrate that increased MCM SUMOylation levels impair genome-wide replication from both early and late origins.

Increasing MCM SUMOylation levels compromises CMG formation

To gain insight into the molecular basis of the replication initiation defects associated with Mcm6-SuOn, we examined CMG formation, because it is critical for replisome assembly. CMG formation can be assessed by measuring the amount of Cdc45 or a GINS subunit (for example, Psf1) that coimmunoprecipitates with Mcm6. Using the samples obtained from experiments depicted in **Figure 5a**, we found that Mcm6-SuOn, compared to Mcm6-ctrl, copurified lower amounts of both Cdc45 and Psf1, at 30 and 40 min after S phase entry (**Fig. 6a**). This finding suggested that Mcm6-SuOn interfered with CMG formation. This conclusion was substantiated by the observation that Mcm4 phosphorylation was reduced in Mcm6-SuOn compared with Mcm6-ctrl cells in G1 and S phases (**Fig. 6b**, lanes 1–8). In addition, we found that mimicking constitutive SUMOylation by using an Mcm6-SUMO fusion led to similar defects as those observed for Mcm6-SuOn; i.e., lower amounts of Cdc45 and Psf1 were associated with Mcm6-SUMO than with the control (**Supplementary Fig. 6a**). Consistently with these results, Mcm6-SUMO fusion strains grew poorly and showed slower replication profiles (**Supplementary Fig. 6b**,**c**). Our findings that increasing MCM SUMOylation through two strategies resulted in similar molecular and phenotypic defects support a negative role for MCM SUMOylation in controlling replication initiation at a step involving CMG formation.

Removing a PP1 cofactor rescues defects in Mcm6-SuOn cells

Because Mcm4 phosphorylation is a prerequisite for CMG formation, we determined whether low Mcm4 phosphorylation might be responsible for the observed Mcm6-SuOn defects. We tested this idea genetically by removing Rif1, a binding partner of phosphatase PP1 (Glc7, essential in budding yeast), because disruption of this complex increases Mcm4 phosphorylation in both G1 and S phases[9–11]. Rif1 loss in Mcm6-SuOn increased Mcm4 phosphorylation without affecting the Mcm6 SUMOylation level in both cell-cycle phases (**Fig. 6b**, lanes 5–12).

Importantly, Rif1 loss improved Mcm6-SuOn growth, as assessed by spore-clone sizes and spotting assays (**Fig. 7a**). Control cells showed wild-type levels of Mcm4 phosphorylation, which were increased by *rif1*Δ, as expected (**Supplementary Fig. 6d**). In addition, we observed no growth defects for Mcm6-ctrl or Mcm6-ctrl *rif1*Δ cells (**Fig. 7a**). We also compared *rif1*Δ with two other mutations, *mcm5-bob1* and $mcm4^{\Delta 2-174}$, which are known to improve replication when Mcm4 phosphorylation is decreased. Although the lethality of Mcm6-ctrl $mcm4^{\Delta 2-174}$ precluded testing of this allele (**Supplementary Fig. 4b**), we found that *mcm5-bob1* did not suppress *cdc7-4* as potently as did *rif1*Δ (**Supplementary Fig. 4c**) and failed to suppress Mcm6-SuOn growth defects (**Supplementary Fig. 4d**), thus suggesting that suppression of Mcm6-SuOn requires maximal bypass of Mcm4 phosphorylation defects. The observed *rif1*Δ suppression of Mcm6-SuOn cells supports the notion that reduced Mcm4 phosphorylation is partly responsible for the replication defects in these cells.

Mcm6-SuOn shows increased association with PP1

The above findings, in conjunction with a previously detected interaction between Glc7 and SUMO[36], raised the possibility that the decreased Mcm4 phosphorylation caused by MCM hyperSUMOylation may be due to increased recruitment of Glc7 to MCM. To test this possibility, we examined the Glc7-Mcm6 association in G1 cells by coimmunoprecipitation. We detected a slight but reproducible enrichment of Glc7 in the immunoprecipitated fraction when Mcm6 was pulled down (**Fig. 7b**). Importantly, we found a two-fold-greater enrichment of Glc7 in the immunoprecipitated fraction of Mcm6-SuOn cells, compared to that of Mcm6-ctrl cells, both in G1 and upon release into S phase (**Fig. 7b** and **Supplementary Fig. 6e**). Because the level of association of Glc7 with Mcm6-SuOn was not affected in cells lacking Rif1 (**Supplementary Fig. 6f**), Rif1 probably has additional roles in promoting Glc7 functions. Together, our results suggest that MCM SUMOylation promotes Glc7 recruitment to MCM, thereby disfavoring MCM phosphorylation.

DISCUSSION

Proper control of replication initiation is important for cell survival and for the prevention of human diseases. Whereas positive regulation promotes origin licensing and replisome assembly, negative regulation is needed to prevent premature initiation or rereplication and to ensure the proper sequence of events in the assembly of functional replisomes. Many of these regulatory targets are subunits of MCM, owing to its central role in multiple aspects of replication. Although phosphorylation is currently the only known chemical modification of MCM that regulates replication initiation, other modifications have recently been identified through studies such as proteomic screens. Here we examined the highly conserved SUMO modification of MCM and demonstrated its temporal and spatial regulation in cells (summarized in **Fig. 7c**). For each MCM subunit, a fraction of the protein showed SUMOylation after Cdc6-mediated MCM loading onto chromatin, before bulk Mcm4 phosphorylation (**Figs. 1** and **2**). As cells entered S phase, Mcm2–6 SUMOylation levels decreased (**Fig. 2**). This loss was associated with replication initiation from both early and late origins (**Fig. 3c**). That the pattern of MCM SUMOylation was opposite from that of replication activity suggested that this modification plays a negative role in replication. We tested this model by increasing MCM SUMOylation through the use of Mcm6-SuOn or mimicking the modification by Mcm6-SUMO fusion (**Fig. 4** and **Supplementary Fig. 6a–c**). In both cases, cell growth and replication were impeded, and CMG levels decreased, thus providing strong evidence for this model (**Figs. 4d** and **5a–e** and **Supplementary Figs. 5** and **6a–c**). In addition, the growth defect of Mcm6-SuOn was rescued either by reducing SUMOylation or diminishing the function of protein phosphatase 1 (PP1), thus restoring Mcm4 phosphorylation (**Figs. 4e**, **6b** and **7a**). Finally, our data suggest that MCM SUMOylation promotes the association of PP1 with MCM (**Fig. 7b** and **Supplementary Fig. 6e**), thereby providing a mechanism for specifically targeting the phosphatase to chromatin-loaded MCM in G1 phase (model in **Fig. 7c**).

Our results also suggest that the reversal of MCM SUMOylation is important. The loss of Mcm2–6 SUMOylation required DDK and GINS (**Fig. 3a**,**b**), thus suggesting that an active deSUMOylation process may occur to remove this replication-inhibition marker. Consistently with the proposal of an active role of DDK in MCM SUMOylation loss, artificially increasing DDK effects by removing Rif1 decreased the SUMOylation of Mcm2 and Mcm6 proteins (**Supplementary Fig. 7a**), although this effect was masked in Mcm6-SuOn cells (**Fig. 6b**). Because SUMOylated forms of Mcm4 did not appear to be phosphorylated (**Supplementary Fig. 7b**), DDK is unlikely to affect deSUMOylation via modulating Mcm4 phosphorylation. Instead, DDK may affect this process by modulating the deSUMOylation enzymes. In depletion studies of the two deSUMOylation enzymes in yeast, we found that acute depletion of Ulp2, but not Ulp1, increased the SUMOylation levels of Mcm4 and 6 on chromatin (**Supplementary Fig. 7c–e**), thus supporting a role of this enzyme in removal of MCM SUMOylation. Thus, although our study focuses on MCM SUMOylation and reveals a role for this modification in counteracting DDK-mediated phosphorylation in G1, the reverse is likely to be true during S phase. Such dual regulation may ensure the precise deployment of each regulatory module during replication initiation. Such dynamic nature of SUMOylation and deSUMOylation in cells, as well as potential SUMOylation loss during extraction probably explain the low levels of SUMOylation observed for each MCM subunit, as for most other substrates. Notably, our data suggest that even a low level of MCM SUMOylation is sufficient to achieve a biological effect, either because SUMOylation promotes the recruitment of an enzyme, a small amount of which can catalyze multiple reactions, or because SUMOylation of multiple MCM subunits may have redundant roles.

Our findings suggest one role of MCM SUMOylation in replication regulation and do not exclude other possible functions. For example, because Rif1 removal only partially rescues the Mcm6-SuOn growth defect (**Fig. 7a**), it is possible that MCM SUMOylation may have other roles in inhibiting replication. One probable scenario is that MCM SUMOylation may disfavor the recruitment of Cdc45 or GINS downstream of the DDK-mediated Mcm4 phosphorylation step (**Fig. 7c**). In addition, SUMOylation of each MCM subunit may have distinct roles. For example, unlike Mcm2–6, Mcm7 SUMOylation persisted throughout most of S phase (**Fig. 2a**,**b**). Given that Mcm7 is the only ubiquitinated MCM subunit that enables MCM removal during replication termination[12], its SUMOylation may be relevant to this event. Our findings regarding one effect of MCM SUMOylation should stimulate future studies to uncover the full scope of the biological effects of this modification.

In summary, our findings reveal that a new SUMO-based regulation exerts a negative influence on MCM activation, thus adding to the known positive regulation conferred by MCM phosphorylation. This dual modulation can expand the range of regulation, allowing for flexible integration of multiple biological cues, including those related to chromatin structure and developmental stages, and providing precision and flexibility in replication regulation. Given that MCM SUMOylation is highly conserved, our work may stimulate the elucidation of the range of effects of this modification in higher organisms.

METHODS

Methods and any associated references are available in the online version of the paper.

Accession codes. Data files have been deposited in the Gene Expression Omnibus database under accession number GSE70407.

Note: Any Supplementary Information and Source Data files are available in the online version of the paper.

ACKNOWLEDGMENTS

We are very grateful to T. Zhang and J. Xiang at the Genomics Resources Core Facility, Weill Cornell Medical College for their kind assistance in genome-wide sequencing analyses. We also thank K. Labib (University of Dundee), D. Shore (Institute of Genetics and Genomics in Geneva), B. Stillman (Cold Spring Harbor Laboratory), J. Diffley (Cancer Research UK London Research Institute), D. Remus (Memorial Sloan Kettering Cancer Center), J. Torres-Rosell (Universitat de Lleida),

M. Kanemaki (Japan National Institute of Genetics) and D. Koshland (University of California, Berkeley) for providing strains, plasmids and antibodies. We also thank Zhao-laboratory members B. Wan for providing reagents and P. Sarangi for discussion. This study was supported by US National Institutes of Health grant GM080670 to X.Z.

AUTHOR CONTRIBUTIONS

L.W. and X.Z. conceived the study and designed the experiments. L.W. performed the experiments. L.W. and X.Z. analyzed the results and wrote the manuscript.

COMPETING FINANCIAL INTERESTS

The authors declare no competing financial interests.

1. Tanaka, S. & Araki, H. Multiple regulatory mechanisms to inhibit untimely initiation of DNA replication are important for stable genome maintenances. *PLoS Genet* **7**, e1002136 (2011).
2. Zegerman, P. & Diffley, J.F.X. Phosphorylation of Sld2 and Sld3 by cyclin-dependent kinases promotes DNA replication in budding yeast. *Nature* **445**, 281–285 (2007).
3. Tanaka, S. *et al.* CDK-dependent phosphorylation of Sld2 and Sld3 initiates DNA replication in budding yeast. *Nature* **445**, 328–332 (2007).
4. Sheu, Y.-J. & Stillman, B. The Dbf4–Cdc7 kinase promotes S phase by alleviating an inhibitory activity in Mcm4. *Nature* **463**, 113–117 (2010).
5. Jackson, A.P., Laskey, R.A. & Coleman, N. Replication proteins and human disease. *Cold Spring Harb. Perspect. Biol.* **6**, 327–342 (2014).
6. Francis, L.I., Randell, J.C.W., Takara, T.J., Uchima, L. & Bell, S.P. Incorporation into the prereplicative complex activates the Mcm2-7 helicase for Cdc7-Dbf4 phosphorylation. *Genes Dev.* **23**, 643–654 (2009).
7. Sheu, Y.-J. & Stillman, B. Cdc7-Dbf4 phosphorylates MCM proteins via a docking site-mediated mechanism to promote S phase progression. *Mol. Cell* **24**, 101–113 (2006).
8. Randell, J.C.W. *et al.* Mec1 is one of multiple kinases that prime the Mcm2-7 helicase for phosphorylation by Cdc7. *Mol. Cell* **40**, 353–363 (2010).
9. Mattarocci, S. *et al.* Rif1 controls DNA replication timing in yeast through the PP1 phosphatase Glc7. *Cell Rep.* **7**, 62–69 (2014).
10. Davé, A., Cooley, C., Garg, M. & Bianchi, A. Protein phosphatase 1 recruitment by Rif1 regulates DNA replication origin firing by counteracting DDK activity. *Cell Rep.* **7**, 53–61 (2014).
11. Hiraga, S. *et al.* Rif1 controls DNA replication by directing Protein Phosphatase 1 to reverse Cdc7-mediated phosphorylation of the MCM complex. *Genes Dev.* **28**, 372–383 (2014).
12. Maric, M., Maculins, T., De Piccoli, G. & Labib, K. Cdc48 and a ubiquitin ligase drive disassembly of the CMG helicase at the end of DNA replication. *Science* **346**, 1253596 (2014).
13. Siddiqui, K., On, K.F. & Diffley, J.F.X. Regulating DNA replication in eukarya. *Cold Spring Harb. Perspect. Biol.* **5**, a012930 (2013).
14. Fragkos, M., Ganier, O., Coulombe, P. & Méchali, M. DNA replication origin activation in space and time. *Nat. Rev. Mol. Cell Biol.* **16**, 360–374 (2015).
15. Yeeles, J.T., Deegan, T.D., Janska, A., Early, A. & Diffley, J.F. Regulated eukaryotic DNA replication origin firing with purified proteins. *Nature* **519**, 431–435 (2015).
16. Heller, R.C. *et al.* Eukaryotic origin-dependent DNA replication *in vitro* reveals sequential action of DDK and S-CDK kinases. *Cell* **146**, 80–91 (2011).
17. Gambus, A. *et al.* GINS maintains association of Cdc45 with MCM in replisome progression complexes at eukaryotic DNA replication forks. *Nat. Cell Biol.* **8**, 358–366 (2006).
18. Morohashi, H., Maculins, T. & Labib, K. The amino-terminal TPR domain of Dia2 tethers SCF(Dia2) to the replisome progression complex. *Curr. Biol.* **19**, 1943–1949 (2009).
19. Cremona, C.A. *et al.* Extensive DNA damage-induced sumoylation contributes to replication and repair and acts in addition to the mec1 checkpoint. *Mol. Cell* **45**, 422–432 (2012).
20. Golebiowski, F. *et al.* System-wide changes to SUMO modifications in response to heat shock. *Sci. Signal.* **2**, ra24 (2009).
21. Elrouby, N. & Coupland, G. Proteome-wide screens for small ubiquitin-like modifier (SUMO) substrates identify *Arabidopsis* proteins implicated in diverse biological processes. *Proc. Natl. Acad. Sci. USA* **107**, 17415–17420 (2010).
22. Geiss-Friedlander, R. & Melchior, F. Concepts in sumoylation: a decade on. *Nat. Rev. Mol. Cell Biol.* **8**, 947–956 (2007).
23. Sarangi, P. & Zhao, X. SUMO-mediated regulation of DNA damage repair and responses. *Trends Biochem. Sci.* **40**, 233–242 (2015).
24. Psakhye, I. & Jentsch, S. Protein group modification and synergy in the SUMO pathway as exemplified in DNA repair. *Cell* **151**, 807–820 (2012).
25. Morris, J.R. *et al.* The SUMO modification pathway is involved in the BRCA1 response to genotoxic stress. *Nature* **462**, 886–890 (2009).
26. Galanty, Y. *et al.* Mammalian SUMO E3-ligases PIAS1 and PIAS4 promote responses to DNA double-strand breaks. *Nature* **462**, 935–939 (2009).
27. Chung, I. & Zhao, X. DNA break-induced sumoylation is enabled by collaboration between a SUMO ligase and the ssDNA-binding complex RPA. *Genes Dev.* **29**, 1593–1598 (2015).
28. Sarangi, P. *et al.* A versatile scaffold contributes to damage survival via sumoylation and nuclease interactions. *Cell Rep.* **9**, 143–152 (2014).
29. Ulrich, H.D. & Davies, A.A. *In vivo* detection and characterization of sumoylation targets in *Saccharomyces cerevisiae*. *Methods Mol. Biol.* **497**, 81–103 (2009).
30. Nishimura, K., Fukagawa, T., Takisawa, H., Kakimoto, T. & Kanemaki, M. An auxin-based degron system for the rapid depletion of proteins in nonplant cells. *Nat. Methods* **6**, 917–922 (2009).
31. Havens, K.A. *et al.* A synthetic approach reveals extensive tunability of auxin signaling. *Plant Physiol.* **160**, 135–142 (2012).
32. Crabbé, L. *et al.* Analysis of replication profiles reveals key role of RFC-Ctf18 in yeast replication stress response. *Nat. Struct. Mol. Biol.* **17**, 1391–1397 (2010).
33. Zegerman, P. & Diffley, J.F.X. Checkpoint-dependent inhibition of DNA replication initiation by Sld3 and Dbf4 phosphorylation. *Nature* **467**, 474–478 (2010).
34. Almedawar, S., Colomina, N., Bermúdez-López, M., Pociño-Merino, I. & Torres-Rosell, J. A SUMO-dependent step during establishment of sister chromatid cohesion. *Curr. Biol.* **22**, 1576–1581 (2012).
35. Mossessova, E. & Lima, C.D. Ulp1-SUMO crystal structure and genetic analysis reveal conserved interactions and a regulatory element essential for cell growth in yeast. *Mol. Cell* **5**, 865–876 (2000).
36. Sung, M.K. *et al.* Genome-wide bimolecular fluorescence complementation analysis of SUMO interactome in yeast. *Genome Res.* **23**, 736–746 (2013).
37. Desdouets, C. *et al.* Evidence for a Cdc6p-independent mitotic resetting event involving DNA polymerase alpha. *EMBO J.* **17**, 4139–4146 (1998).
38. Hawkins, M. *et al.* High-resolution replication profiles define the stochastic nature of genome replication initiation and termination. *Cell Rep.* **5**, 1132–1141 (2013).

ONLINE METHODS

Yeast strains and techniques. Standard procedures were used in cell growth and medium preparation. Strains were isogenic to W1588-4C, a *RAD5* derivative of W303 (*MATa ade2-1 can1-100 ura3-1 his3-11,15 leu2-3,112 trp1-1 rad5-535*)[39]. Strains and their usage in specific figure panels are listed in **Supplementary Table 1**. Proteins were tagged at their endogenous loci by standard methods, and correct tagging was verified by sequencing. Each MCM subunit was tagged with a triple HA tag at the C terminus, except Mcm3, which was tagged at its N terminus and expressed from the ADH1 promoter. The P_{ADH1}-Mcm3-HA expression level was about half that of Mcm7-HA (**Supplementary Fig. 7f**), consistently with their endogenous protein level ratio[40] and indicating normal protein levels. Mcm5 was additionally tagged with the Strep tag II at its C terminus (**Figs. 1d** and **3b**). Aid-tagging has been described previously[30,31]. In brief, Psf2 was fused with a 3V5 tag-IAA7 module at its C terminus, and Mcm6 was fused with IAA17-3Flag at its C terminus. Mcm6-SuOn and Mcm6-ctrl were constructed as described with minor modifications[34]. Both tags and a 3V5 linker were fused to the C terminus of Mcm6. SuOn is composed of the catalytically dead Ulp1 protease domain (amino acids 418–621, with C580S abolishing the activity)[34,35]. The control tag contained the F474A mutation, which disrupts SUMO interaction[34,35]. SuOn is different from the canonical SUMO-interacting motif (SIM) because it interacts with the C-terminal tail of SUMO through a distinct large interface and has strict orientation requirements[35]. Yeast dissection and spotting assays were performed with standard procedures. All genetic and biochemical experiments were performed with two different spore clones for each genotype.

Synchronization procedures. For experiments that entailed alpha-factor arrest, cells were treated for 2.5 h with 5 μg/ml (for *BAR1*$^+$ cells) or 100 ng/ml (for *bar1Δ* cells) alpha factor. For experiments involving G2-M arrest, cells were grown in medium containing 1% DMSO to early log phase and were treated with 15 μg/ml nocodazole for 3 h. In all cases, cell morphology was verified to confirm the arrest. Experiments in **Figures 1d** and **4c** were performed as described previously[37]. In brief, cultures grown at 24 °C were arrested in G2-M and split into two groups, one of which received 2% glucose for 1 h. Subsequently, cells were released into the same medium containing alpha factor for 2.5 h before harvesting. For the experiment in **Figure 3a**, cells were arrested by alpha factor at 24 °C, and then the temperature was shifted to 37 °C for 1 h. Subsequently, cultures were split into two groups, only one of which was released from alpha factor into S phase. Samples were taken from both cultures 40 min afterward. For experiments in **Figure 3b**, cells were arrested in G2-M phase at 24 °C, and IAA was added to a final concentration of 1 mM. After 1 h, cells were released into medium containing alpha factor and 1 mM IAA for 3 h and then released into medium containing 1 mM IAA for 40 min. For the experiment in **Figure 3c**, alpha factor–arrested cells were released into YPD medium containing 300 μg/ml pronase and 200 mM HU at 24 °C for 40 min. For experiments in **Figures 5** and **6a**, diploid cells containing Mcm6-SuOn or Mcm6-ctrl and an Mcm6-aid degron allele and which were homozygous for *cdc7-4* were used. Cells were grown at the permissive temperature for *cdc7-4* (24 °C) and synchronized in G2-M. Then Mcm6-aid was depleted by the addition of 1 mM IAA for 1 h. Subsequently, cells were released from G2-M arrest and synchronized at the G1-S boundary by raising the temperature to 37 °C to inactivate *cdc7-4*. Finally, cells were released by rapid cooling to 24 °C.

Detection of protein SUMOylation. Unless otherwise indicated, the standard Ni-NTA pulldown method was used as previously described[29]. Smt3 was tagged with HF (His_6-Flag) at its N terminus and expressed from its endogenous promoter[41]. Cell extracts prepared by 55% TCA precipitation were dissolved in buffer A (6 M guanidine HCl, 100 mM sodium phosphate, pH 8.0, and 10 mM Tris-HCl, pH 8.0) with rotation at room temperature. Cleared supernatant was then incubated with Ni-NTA resin (Qiagen) after the addition of Tween 20 (0.05% final concentration) and imidazole (4.4 mM final concentration) overnight at room temperature. Beads were then washed twice with buffer A containing 0.05% Tween 20 and four times with buffer C (8 M urea, 100 mM sodium phosphate, pH 6.3, and 10 mM Tris-HCl, pH 6.3) containing 0.05% Tween 20. HU buffer (8 M urea, 200 mM Tris-HCl, pH 6.8, 1 mM EDTA, 5% SDS, 0.1% bromophenol blue, 1.5% DTT, and 200 mM imidazole) was used to elute proteins from the beads. Samples were loaded onto a 3–8% gradient Tris-acetate gel (Life Technologies). Western blots were probed with antibodies recognizing the tagged substrates detecting both SUMOylated and unmodified bands. The unmodified bands were due to nonspecific binding to the Ni-NTA beads and were not enriched in samples from cells expressing HF-Smt3. Our previous work with a protein immunoprecipitation method has indicated SUMOylation of two MCM subunits under normal growth conditions[19], and we also demonstrated SUMOylation of additional MCM subunits with this method (**Supplementary Fig. 1b**). Because deSUMOylation cannot be efficiently prevented during this procedure, weakly abundant SUMOylation forms are difficult to detect. However, the use of both untagged and HF-SUMO allowed better assessment of SUMOylation, owing to the different sizes of SUMOylated forms in the two situations (**Supplementary Fig. 1b**).

Two-dimensional agarose gel electrophoresis (2D gel). 2D gel analyses were performed as previously described[42]. Genomic DNA was extracted from spheroplasts and purified by standard CsCl centrifugation at 90,000 r.p.m. for 9 h at 15 °C. DNA was digested by EcoRI and separated by agarose gel electrophoresis in two dimensions. DNA was transferred to Hybond-XL membrane (GE Healthcare) and analyzed by Southern blot hybridization with probes specific for ARS305 or ARS609, as described previously[43]. Primer sequences used for amplification of the probes are available upon request.

Whole-genome sequencing and copy-number calculation. Both procedures were carried out as previously described[38,44]. Mcm6-ctrl and Mcm6-SuOn cells were collected at 0 and 30 min (as described in **Fig. 5a**). 1.5 μg genomic DNA from each sample was used to generate libraries with a KAPA library kit (iGO facility, Memorial Sloan Kettering Cancer Center) and sequenced with a HiSeq 2500 (Illumina). At least 10 million 50-bp paired-end reads were generated per sample. Reads were mapped to the S288c reference genome (SGD, SacCer2), excluding repetitive sequences, and were summed in 1-kb bins with Genome Browser. Bins containing fewer than 600 reads were excluded. Custom R script was used to analyze the value for each locus. In brief, for each strain, the binned reads from the 30-min sample at a given locus were divided by those from the 0-min sample and normalized to the ratio of total reads, thus yielding a genome-wide mean value of 1. This number was adjusted by the relative DNA content at 30 min in the FACS fitting curve (**Fig. 5b**) to derive a relative copy number of the particular locus. The maps of adjusted copy numbers were further smoothed with the LOESS function (**Fig. 5e** and **Supplementary Fig. 5**). Detailed methods and data for calculating the relative copy number on the basis of whole-genome sequencing are included in the GEO database (GSE70407).

Protein extraction and immunoprecipitation (IP). For **Figures 2b** and **6a**, cells were resuspended in IP buffer (100 mM HEPES/KOH, pH 7.9, 100 mM KOAC, 2 mM MgOAC, 1 mM ATP, 1% Triton X-100, 2 mM NaF, 0.1 mM Na_3VO_4, 20 mM β-glycerophosphate, 1 mM PMSF, 10 mM benzamidine HCl, 10 μg/ml leupeptin, and 1 μg/ml pepstatin A) containing 1× protease inhibitors (EDTA-free, Roche) and 20 mM NEM. Cells were disrupted by bead-beating. Benzonase was added to cell lysates, which were incubated for 1 h at 4 °C. After centrifugation for 20 min at 15,000 r.p.m. at 4 °C, the supernatant was collected and incubated with prewashed HA (26182, Fisher) or V5-conjugated beads (A7345, Sigma-Aldrich) for 2 h at 4 °C. For **Figure 7b**, minor changes were made to the IP buffer: 50 mM HEPES/KOH, pH 7.9, and 150 mM KOAC was used, and glycerol was added at a final concentration of 10%.

Immunoblotting analysis and antibodies. Protein samples were resolved by 3–8% or 4–20% gradient gels (Life Technologies and Bio-Rad) and transferred to a 0.2-μm nitrocellulose membrane (G5678144, GE). Antibodies used were anti-HA (F-7, Sc-7392, Santa Cruz Biotechnology), anti-V5 (R960-25, Invitrogen), anti-myc (9E10, Bio X cell), PAP (P1291, Sigma), anti-flag (M2, Sigma), anti-Rad53 (yC-19, sc-6749, Santa Cruz Biotechnology), anti-Orc2 (SB46, Abcam), anti-Pgk1 (22C5D8, Invitrogen), anti-Cdc6 (9H8/5, Abcam), anti-Strep tag II (A01732, Genscript), anti-Psf1 and anti-Mcm6 (gifts from K. Labib)[17], anti-Orc6 and anti-Cdc45 (gifts from B. Stillman)[4] and anti-SUMO[39]. Validation of these antibodies is provided either on the manufacturers' websites or in the cited references. For quantification purposes, membranes were scanned with a Fujifilm LAS-3000 luminescent image analyzer, which has a linear dynamic range of 10^4. Quantification of blots and generation of figures was performed with ImageGauge and Photoshop.

Lambda phosphatase treatment. After immunoprecipitation with anti-HA antibody–conjugated beads (Fisher, 26182) or Ni-NTA beads (Qiagen), the beads were washed three times with wash buffer (50 mM K-HEPES, pH 7.9, 150 mM KOAC, 2 mM MgOAC, 10 µg/ml pepstatin, 10 µg/ml leupeptin, 0.5 mM PMSF, 1 mM benzamidine and 20 mM NEM). Beads were then resuspended in lambda phosphatase reaction buffer (1× NEBuffer for PMP, 1 mM $MnCl_2$ and 10 µg/ml pepstatin, 10 µg/ml leupeptin, 0.5 mM PMSF, 1 mM benzamidine and 20 mM NEM). In control tests, the beads were incubated with reaction buffer and phosphatase inhibitors (50 mM EDTA, 50 mM NaF and 10 mM Na_3VO_4). 80 U of lambda phosphatase (NEB, P0753S) was added, and incubated at 30 °C for 30 min. Laemmli buffer was added to stop the reaction, and the proteins were eluted by boiling at 95 °C for 5 min before SDS-PAGE and western blotting analysis.

Other methods. Chromatin fractionation was performed as described previously with minor modifications[45]. In brief, spheroplasts were lysed in lysis buffer containing 1% Triton X-100 and were laid upon a 30% sucrose cushion and centrifuged at 13,000 r.p.m. for 20 min to separate the supernatant and chromatin fractions. The chromatin-bound fraction was washed once with lysis buffer and resuspended in the same buffer. Equal volumes of samples from lysate, supernatant and chromatin fractions were precipitated with 20% TCA and resuspended in Laemmli buffer with the addition of 2M Tris to neutralize TCA. Flow cytometry was performed as previously described with a FACSCalibur flow cytometer, and data were analyzed with FlowJo Software. To calculate the relative DNA content in **Figure 5b**, the distance between 1N and 2N DNA peaks was considered to be 2, and the position of the 1N peak was considered to be 1. Then the distance between DNA peaks at each time point and the 1N DNA peak in G1 cells was measured and scaled between 1 and 2 and plotted. Original images of gels and blots used in this study can be found in **Supplementary Data Set 1**.

39. Zhao, X. & Blobel, G. A SUMO ligase is part of a nuclear multiprotein complex that affects DNA repair and chromosomal organization. *Proc. Natl. Acad. Sci. USA* **102**, 4777–4782 (2005).
40. Donovan, S., Harwood, J., Drury, L.S. & Diffley, J.F. Cdc6p-dependent loading of Mcm proteins onto pre-replicative chromatin in budding yeast. *Proc. Natl. Acad. Sci. USA* **94**, 5611–5616 (1997).
41. Takahashi, Y. *et al.* Cooperation of sumoylated chromosomal proteins in rDNA maintenance. *PLoS Genet.* **4**, e1000215 (2008).
42. Friedman, K.L. & Brewer, B.J. Analysis of replication intermediates by two-dimensional agarose gel electrophoresis. *Methods Enzymol.* **262**, 613–627 (1995).
43. Hang, L.E. *et al.* Rtt107 Is a multi-functional scaffold supporting replication progression with partner sUMO and ubiquitin ligases. *Mol. Cell* **60**, 268–279 (2015).
44. Murakami, H. & Keeney, S. Temporospatial coordination of meiotic DNA replication and recombination via DDK recruitment to replisomes. *Cell* **158**, 861–873 (2014).
45. Schepers, A. & Diffley, J.F. Mutational analysis of conserved sequence motifs in the budding yeast Cdc6 protein. *J. Mol. Biol.* **308**, 597–608 (2001).

doi:10.1038/nsmb.3173